Taylor & Francis
Taylor & Francis Group

REPORT

OPEN ACCESS

Check for updates

Structure-based engineering to restore high affinity binding of an isoform-selective anti-TGFβ1 antibody

Dana M. Lord [a],*, Julie J. Bird [a],*, Denise M. Honey[a], Annie Best[b], Anna Park [a], Ronnie R. Wei [a], and Huawei Qiu[a]

[a]Biologics Research, Sanofi, Framingham, MA, USA; [b]Biopharmaceutics Development, Sanofi, Framingham, MA, USA

ABSTRACT

Metelimumab (CAT192) is a human IgG4 monoclonal antibody developed as a TGFβ1-specific antagonist. It was tested in clinical trials for the treatment of scleroderma but later terminated due to lack of efficacy. Subsequent characterization of CAT192 indicated that its TGFβ1 binding affinity was reduced by ~50-fold upon conversion from the parental single-chain variable fragment (scFv) to IgG4. We hypothesized this result was due to decreased conformational flexibility of the IgG that could be altered via engineering. Therefore, we designed insertion mutants in the elbow region and screened for binding and potency. Our results indicated that increasing the elbow region linker length in each chain successfully restored the isoform-specific and high affinity binding of CAT192 to TGFβ1. The crystal structure of the high binding affinity mutant displays large conformational rearrangements of the variable domains compared to the wild-type antigen-binding fragment (Fab) and the low binding affinity mutants. Insertion of two glycines in both the heavy and light chain elbow regions provided sufficient flexibility for the variable domains to extend further apart than the wild-type Fab, and allow the CDR3s to make additional interactions not seen in the wild-type Fab structure. These interactions coupled with the dramatic conformational changes provide a possible explanation of how the scFv and elbow-engineered Fabs bind TGFβ1 with high affinity. This study demonstrates the benefits of re-examining both structure and function when converting scFv to IgG molecules, and highlights the potential of structure-based engineering to produce fully functional antibodies.

Introduction

Transforming growth factor β (TGFβ) is a multifunctional cytokine that controls a wide array of biological processes, including cellular proliferation, differentiation, migration and apoptosis.[1] With such an extensive role in the cell, TGFβ has been linked to several diseases when it is not properly regulated. For instance, an increased level of TGFβ in tissues is believed to be a factor in the development of idiopathic pulmonary fibrosis and myocardial fibrosis.[2,3] Furthermore, TGFβ has been linked to solid and hematopoietic tumors.[4] As an inhibitor of cell growth, TGFβ has a pro-apoptotic effect on tumor cells, thus acting as a tumor suppressor. However, many tumor cells respond to TGFβ as an oncogenic factor. Therefore, TGFβ may act as a tumor suppressor or a pro-tumorigenic factor depending on tumor type and stage.[4,5]

There are three TGFβ isoforms in humans (TGFβ1, TGFβ2, and TGFβ3), which all signal through the same serine/threonine kinase type I and type II cell surface receptors.[4,6] While having similar cellular targets, biological studies have demonstrated that the isoforms have different expression profiles. Of the three isoforms, TGFβ1 is the most abundant and ubiquitously expressed.[4] Metelimumab, also known as CAT192, is a human IgG4 monoclonal antibody that was designed to selectively neutralize TGFβ1. CAT192 was tested for the treatment of diffuse cutaneous systemic sclerosis, also known as scleroderma, but demonstrated insufficient efficacy.[7]

The elbow region of an antibody is a linker that joins the variable domains (VL and VH) and the constant domains (CL and CH1) of the molecule's antigen-binding fragment (Fab).[8] The range of flexibility of the elbow region in an IgG molecule allows the Fab arms to adopt a range of angles, which permits binding to epitopes that are separated by certain distances.[9,10] It was also demonstrated that the elbow region can be an important functional element of antibody structure, and that integrity of the joint between variable and constant domains is essential for complete activity of a humanized antibody.[11] CAT192, however, was derived from a scFv library, and variable domains in a scFv molecule are joined directly by a linker that is typically longer than a Fab elbow region.[12,13] The longer linker in the scFv may allow the variable domains to be separated in a conformation that is not possible in the restricted elbow region of the Fab molecule.

We aimed to engineer the flexibility/affinity back in the Fab or IgG versions of the CAT192 scFv by adding additional amino acids in the elbow region. These constructs with varying linker

---

*These authors contributed equally to this work.

lengths were analyzed for their affinity, efficacy, and thermal stability. The crystal structures were determined for selected constructs to demonstrate the conformational changes of the engineered antibodies. This study shows that engineering an ideal number of residues into the elbow region can restore the binding affinity that is lost during the scFv to IgG conversion.

Results

Binding studies of CAT192 scFv and IgG

Biacore experiments showed CAT192 scFv to bind TGFβ1 at 2.8 ± 1.41 nM (Fig. 1A), whereas no binding was detected against TGFβ2 or TGFβ3 (Supplementary Fig. 1A). However, when CAT192 scFv was converted to IgG4, a significant decrease in affinity to TGFβ1 was observed (K_D = 138.6 ± 33.51 nM) (Fig. 1B). In addition, conversion to IgG1 or Fab also displayed very weak binding to TGFβ1 (Fig. 1C and 1D), showing K_Ds of 524 nM and 443 nM, respectively. This indicates that the subtype and Fc format was not responsible for this phenomenon. The CAT192 single-chain molecule contains a long (SSGGGSGGGGSGGGGS) linker connecting the heavy and light chain Fv domains. This flexible linker is lost in the conversion to IgG. A slight improvement in TGFβ1 binding was observed when CAT192 was treated with urea, suggesting that conformation change or flexibility may play a role in the observed affinity differences (Supplementary Fig. 1C).

Design and characterization of CAT192 Fab variants

Site-directed mutagenesis was performed aiming to introduce flexibility into the Fab versions. For the first round of Fab mutations, additional amino acids were inserted in the light chain (LC) elbow region. More specifically, mutants were designed to add one glycine (L1), two glycines (L2), two glycines and one serine (L3), three glycines and one serine (L4), and four glycines and one serine (L5) sequences into the wild type (WT) light chain elbow region (Table 1). The light chain mutants bound to TGFβ1 with a significantly increased affinity compared to the WT CAT192 Fab (Table 2). These results show a step-wise improvement in TGFβ1 binding with the insertion of each additional residue into the elbow region of the Fab. None of the CAT192 LC Fab mutants bound to TGFβ2 or TGFβ3 (result not shown), demonstrating that the mutants retained isoform-selectivity.

For the second round of mutations, constructs were designed inserting additional amino acids in the heavy chain (HC) elbow region of CAT192 Fab. Like the light chain mutants, either one glycine (H1), two glycines (H2), or four glycines and a serine (H5) sequences were added into the wild-type heavy chain elbow region (Table 1). The results (Table 2) show that addition of amino acids in the elbow region of CAT192 HC also improves TGFβ1 binding. Like the light chain mutants, these mutants were also shown to be isoform-specific (result not shown).

Since the binding affinity of CAT192 Fab to TGFβ1 improved with insertion of additional amino acids into the elbow regions of the HC or LC, different HC and LC mutant combinations were tested next. Twenty-three variants plus WT were tested for their binding affinity to TGFβ1 (Table 2, Fig. 2). Combining the HC and LC insertion mutants also restored TGFβ1 binding affinity; however, there was a saturation effect with the number of insertions. For example, the combination of "HC+G" and "LC+GG" (H1/L2) mutants showed one of the highest affinity binding (2.6 nM) to TGFβ1, which was the same as combining the "HC+GGGGS" and "LC+GGGGS" (H5/L5) insertions (Table 2).

Affinity and potency characterization of IgG4 variants

The HC and LC insertion mutants were converted to an IgG4 format in order to confirm that the affinity to TGFβ1
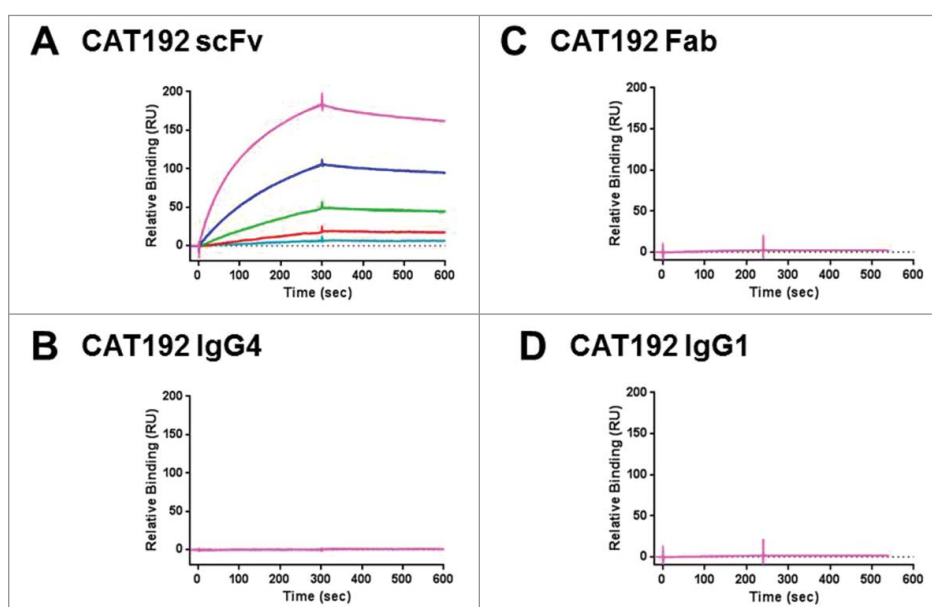
Figure 1. Comparison of TGFβ1 binding between CAT192 constructs. (A) Sensorgrams of CAT192 scFv binding to immobilized TGFβ1 (262RU) for 5 different concentrations in duplicate: 30, 10, 3.3, 1.1, and 0.4 nM. (B) Sensorgrams of CAT192 IgG4 (metelimumab), (C) CAT192 Fab, and (D) CAT192 IgG1 for one 30 nM concentration in duplicate.

Table 1. Modified light chain & heavy chain elbow region insertion variants.

Name	Insertion	Position	Amino acid sequence
L0	WT LC	Light chain elbow region	LEIKRTVA
L1	LC+G	Light chain elbow region	LEIKGRTVA
L2	LC+GG	Light chain elbow region	LEIKGGRTVA
L3	LC+GGS	Light chain elbow region	LEIKGGSRTVA
L4	LC+GGGS	Light chain elbow region	LEIKGGGSRTVA
L5	LC+GGGGS	Light chain elbow region	LEIKGGGGSRTVA
H0	WT HC	Heavy chain elbow region	TVTVSSAST
H1	HC+G	Heavy chain elbow region	TVTVSGSAST
H2	HC+GG	Heavy chain elbow region	TVTVSGGSAST
H5	HC+GGGGS	Heavy chain elbow region	TVTVSGGGGSSAST

was regained. The H2/L2 mutant was also included for comparison with the single-arm insertion mutants. Surface plasmon resonance (SPR) analysis of the CAT192 IgG4 insertion mutants agrees with the Fab mutant results that TGFβ1 binding affinity is regained when amino acids are added to the elbow regions of the heavy and light chains (H2/L2 IgG4 K_D = 0.2 nM). None of the mutants were seen to bind TGFβ2 or TGFβ3 (Supplementary Fig. 2). The regained affinity for H2/L2 IgG4 is within the range of known therapeutic TGFβ antibodies, such as fresolimumab (K_D = 1.7 nM).[14]

The CAT192 IgG4 insertion mutants were then characterized in an A549 bioassay to measure the TGFβ1 neutralization activity.[15] The potency assay is based on the TGFβ-induced release of interleukin-11 (IL-11) by the human lung epithelial cell line A549. When one glycine was added to the LC, the potency of CAT192 to neutralize TGFβ1-stimulated IL-11 production was improved compared with the weak activity demonstrated by CAT192 WT (Fig. 3A). Addition of one glycine in the HC had a greater effect on the potency of CAT192 than when it was added in the LC (Fig. 3B). Among the tested mutants, the H2/L2 mutant had the highest potency (Fig. 3B).

Stability assessment of CAT192 insertion variants

Differential scanning fluorimetry (DSF) was performed on the insertion mutants to determine how the additional amino acids at the elbow region affected thermostability. Melting temperatures (T_ms) were calculated from the unfolding patterns of each mutant, and are shown in Fig. 4. The results show that the relative stability of the CAT192 Fab insertion mutants decreases slightly with the insertion of additional residues in the elbow regions of the heavy and light chains. The T_ms of some of the longer chain mutants could not be calculated due to the unfolding pattern. Slight decreases in stability was also observed when some of the light chain mutants were converted from Fab into the IgG4 format (Fig. 4B).

Structural analysis of CAT192 Fab variants

To understand how each elbow length affected binding, the structures of multiple CAT192 elbow variant Fabs with varying affinities to TGFβ1 were solved using x-ray crystallography. The constructs chosen were WT CAT192 (H0/L0), a low binding affinity mutant (H0/L1), a moderate binding affinity mutant (H5/L0), and a high binding affinity mutant (H2/L2). Wild type, H0/L1, and H5/L0 all crystalized similarly in a PEG condition at neutral pH. Conversely, H2/L2 only crystallized in an ammonium sulfate condition and in a more acidic pH (Table 3).

Superposition of each Fab on the constant domain shows dramatic conformational changes between the high affinity mutant and the other lower binding affinity Fab constructs. While the relative orientations of the variable domain consistently differ between H2/L2 and the other crystallized constructs, the other variants (H0/L1 and H5/L0) show a similar orientation to wild type (Fig. 5). The WT Fab and the two other low/moderate binding affinity structures show little variation and superimpose with WT with an overall root-mean-square

Table 2. TGFβ1-binding affinity of the heavy and light Chain combination mutants determined by biacore.

Fabs	Variant Name	Antigen	k_a (x10^5 M^{-1}s^{-1})	k_d (x10^{-4} s^{-1})	K_D (nM)
WT HC/WT LC	H0/L0	TGFβ1	n/a	n/a	n/a
WT HC/LC+G	H0/L1	TGFβ1	n/a	n/a	n/a
WT HC/LC+GG	H0/L2	TGFβ1	0.7 ± 0.06	4.9 ± 1.05	7.4 ± 0.93
WT HC/LC+GGS	H0/L3	TGFβ1	0.8 ± 0.15	4.7 ± 1.72	6.4 ± 3.44
WT HC/LC+GGGS	H0/L4	TGFβ1	1.5 ± 0.90	5.7 ± 0.21	4.6 ± 2.84
WT HC/LC+GGGGS	H0/L5	TGFβ1	1.0 ± 0.21	4.8 ± 1.50	4.6 ± 0.58
HC+G/WT LC	H1/L0	TGFβ1	n/a	n/a	n/a
HC+G/LC+G	H1/L1	TGFβ1	1.3 ± 0.33	5.3 ± 1.51	4.1 ± 0.13
HC+G/LC+GG	H1/L2	TGFβ1	2.1 ± 0.41	5.4 ± 1.73	2.6 ± 0.31
HC+G/LC+GGS	H1/L3	TGFβ1	2.0 ± 0.42	5.5 ± 2.02	2.8 ± 0.45
HC+G/LC+GGGS	H1/L4	TGFβ1	2.3 ± 0.41	5.4 ± 2.16	2.3 ± 0.52
HC+G/LC+GGGGS	H1/L5	TGFβ1	2.3 ± 0.50	5.5 ± 1.95	2.4 ± 0.30
HC+GG/WT LC	H2/L0	TGFβ1	0.5 ± 0.44	7.7 ± 0.63	20.7 ± 15.63
HC+GG/LC+G	H2/L1	TGFβ1	1.2 ± 0.15	5.4 ± 0.69	4.5 ± 0.05
HC+GG/LC+GG	H2/L2	TGFβ1	2.1 ± 0.11	5.2 ± 1.98	2.5 ± 1.10
HC+GG/LC+GGS	H2/L3	TGFβ1	2.0 ± 0.20	5.5 ± 1.70	2.8 ± 0.62
HC+GG/LC+GGGS	H2/L4	TGFβ1	1.9 ± 0.67	5.0 ± 1.82	2.9 ± 1.95
HC+GG/LC+GGGGS	H2/L5	TGFβ1	2.4 ± 0.21	5.6 ± 2.28	2.3 ± 0.78
HC+GGGGS/WT LC	H5/L0	TGFβ1	0.6 ± 0.16	4.9 ± 1.26	8.7 ± 0.29
HC+GGGGS/LC+G	H5/L1	TGFβ1	2.0 ± 0.31	5.4 ± 1.99	2.7 ± 0.61
HC+GGGGS/LC+GG	H5/L2	TGFβ1	2.5 ± 0.28	5.7 ± 2.29	2.3 ± 0.64
HC+GGGGS/LC+GGS	H5/L3	TGFβ1	2.3 ± 0.54	5.8 ± 1.85	2.6 ± 0.21
HC+GGGGS/LC+GGGS	H5/L4	TGFβ1	2.5 ± 0.46	5.8 ± 1.99	2.3 ± 0.40
HC+GGGGS/LC+GGGGS	H5/L5	TGFβ1	2.3 ± 0.49	6.0 ± 2.10	2.6 ± 0.35
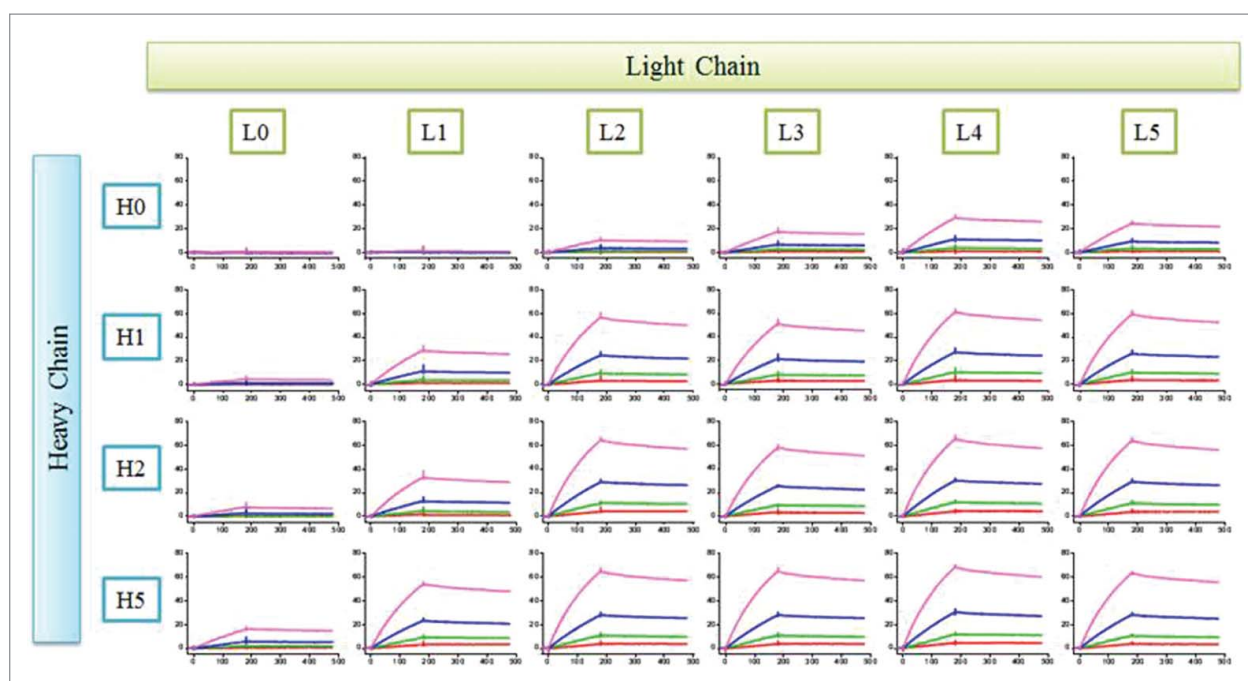
Figure 2. TGFβ1 binding of CAT192 Fab variants. TGFβ1 binding sensorgrams of CAT192 Fabs with amino acid insertions made on the light chain, heavy chain, or both. Four different concentrations of Fab (30, 10, 3.3, and 1.1 nM) were injected over immobilized TGFβ1 (100 RU).

deviation (R.M.S.D.) of 0.507Å and 0.545Å for H0/L1 and H5/L0, respectively. In contrast, WT CAT192 and H2/L2 superimpose with a R.M.S.D. of 8.941Å (Fig. 6A).

The H2/L2 elbow insertion also brings about large changes in the antigen binding interface. While the variable domains of WT CAT192 cover a distance of ~50Å (Fig. 6B), the rotation of the variable domains in H2/L2 causes the domains to display a distance of 70Å between the same residues (Fig. 6C). This length is measured from two distal residues: HC S75 and LC G16. Furthermore, in the WT structure, the distance between HC and LC complementary-determining regions (CDRs) are 27Å, 22Å, and 16Å for CDR1, CDR2, and CDR3, respectively (Fig. 6B). With the H2/L2 elbow insertion, the CDR3s are much closer at a distance of 10Å, while CDR1s are 25Å apart and CDR2s are 36Å apart. The closer association of the CDR3 loops in the high binding affinity mutant allows CDRH3 to make additional hydrophobic interactions and hydrogen bonds with CDRL3. This CDR3 interface may be important for binding to the TGFβ1 epitope. Furthermore, the high

binding affinity H2/L2 structure is the only CAT192 Fab structure where the CDRH3 region is completely ordered.

Discussion

Antibody re-formatting from parental scFv and Fab to IgG is a common practice in antibody research and development. It has been demonstrated that phage display-based affinity maturation of IgGs could be dependent on the antibody format employed for selection and screening.[16] A problem that may be commonly seen during antibody generation, but not always reported, is the loss of antigen binding affinity during these scFv to IgG conversions.[17-19] This was observed when CAT192 scFv was converted to CAT192 Fab and IgG4. CAT192 IgG4 displayed a significant decrease in K_D compared to CAT192 scFv (K_D = 138.6 nM vs. 2.8 nM). This low affinity is characterized by a very slow on-rate (k_a = 0.01 × 10^5 $M^{-1}s^{-1}$) and off-rate (k_d = 0.15 × 10^{-4} s^{-1}). One explanation of the slow on-rate could be that TGFβ1 may require a potential induced fit conformational change, and, once bound, the complex is stable,
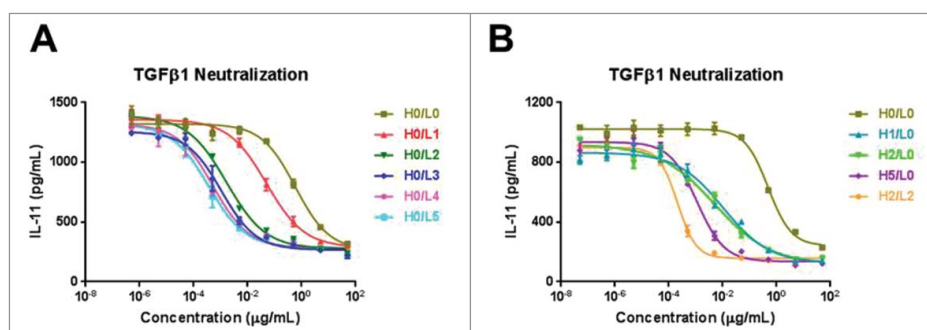
Figure 3. Cell potency of CAT192 mutants. Inhibitory effects by the CAT192 IgG4 (A) light chain insertion mutants and (B) heavy chain mutants/combination mutant on TGFβ1-stimulated IL-11 production in an A549 cell potency assay.

**Table 3.** Data collection and refinement statistics for CAT192 Fab variants.

	H0/L0	H0/L1	H5/L0	H2/L2
Condition	12% PEG 8K, 0.1 M Sodium cacodylate pH 6.0, 0.2 M MgCl$_2$	20% PEG 8K, 0.1 M Sodium cacodylate pH 6.5, 0.2 M MgCl$_2$	10.3% PEG 20K, 0.0938 MMES pH 6.0, 2.5% DMSO	2 M Ammonium sulfate, 0.1 Msodium acetate trihydrate pH 4.6
Wavelength (Å)	1.54	1.54	1.54	1.54
Resolution	45.38–2.49 (2.62–2.49)	48.22–2.80 (2.95–2.80)	46.37–2.45 (2.58–2.45)	45.11–2.35 (2.48–2.35)
R_{merge}	0.097 (0.396)	0.162 (0.497)	0.123 (0.443)	0.098 (0.332)
Total # observations	114301 (13879)	45458 (6534)	131699 (15014)	59391 (7335)
# unique observations	32736 (4715)	12665 (1837)	36551 (5019)	16309 (2164)
I/sig	8.8 (2.3)	5.3 (2.4)	7.4 (2.2)	8.6 (2.9)
Completeness (%)	99.7 (98.8)	99.99 (100)	98.9 (93.7)	93.2 (85.1)
Redundancy	3.5 (2.9)	3.6 (3.6)	3.6 (3.0)	3.6 (3.4)
Space group	P2$_1$	I 121	P2$_1$	C2
Unit Cell				
a, b, c (Å)	55.95 83.35 104.91	72.79 65.72 110.45	54.44 83.89 112.25	109.06 86.59 45.89
α, β, γ (°)	90.00 104.77 90.00	90.00 102.83 90.00	90.00 97.49 90.00	90.00 100.57 90.00
Molecules per ASU	2	1	2	1
R_{work}	0.21	0.25	0.18	0.21
R_{free}	0.26	0.30	0.24	0.26
RMS(bonds)	0.00	0.01	0.00	0.00
RMS(angles)	0.47	0.81	0.56	0.48
Clashscore	4.88	13.93	4.13	2.03
Ramachandran favored (%)	96.34	94.72	96.77	95.47
Ramachandran outliers (%)	0.24	0.24	0.24	0.00
Rotamer outliers (%)	0.70	0.00	0.00	0.00
PDB	6AMJ	6AMM	6ANP	6AO0

Statistics for the highest-resolution shell are shown in parentheses.

as characterized by a very slow off-rate. The scFv contains much more structural flexibility between its variable domains because the domains are joined by a large linker. However, the Fab and IgG molecules are subject to the constraints of the elbow linker that anchor the variable domains. Thus, we proposed and tested the hypothesis in this study that the ability of the variable domains to adopt different conformations, due to different structural constraints in scFv and Fab/IgG, can have an impact on binding affinity.

The flexibility of the elbow region allows the Fab arm to adopt a certain range of angles, which allows binding to epitopes whose variable domains are spaced certain distances apart. In this study, site-directed mutagenesis was performed on the CAT192 elbow regions to improve TGFβ1 binding affinity. This strategy was supported by a study where the elbow angles for 365 different Fabs were studied and compared.[13] Standfield *et al.* observed that λ light chains adopt a wider range of elbow angles compared to κ light chains. The authors proposed that the hyperflexibility in the λ light chain may be due to an insertion in their elbow region, which was one residue longer than in κ chains and typically a glycine. Our study theorized that the elbow region in CAT192 Fab or IgG4 needs to be relaxed to allow an extended conformation between the variable domains (such as seen in the scFv). The wild type CAT192 constructs had the weakest binding affinity for TGFβ1 in this study. For the antibodies with wild type HC/LC insertions, the affinity increased with additional residues added in the light chain. For the reverse antibody combination (wild type LC/HC insertions), affinity also increased with additional residues in the elbow region. This demonstrates that affinity increases with additional flexibility introduced into each chain. Interestingly, for the combination HC/LC insertion mutants, saturation was reached in terms of affinity. The affinity did not improve drastically after two glycines were introduced into each chain at the
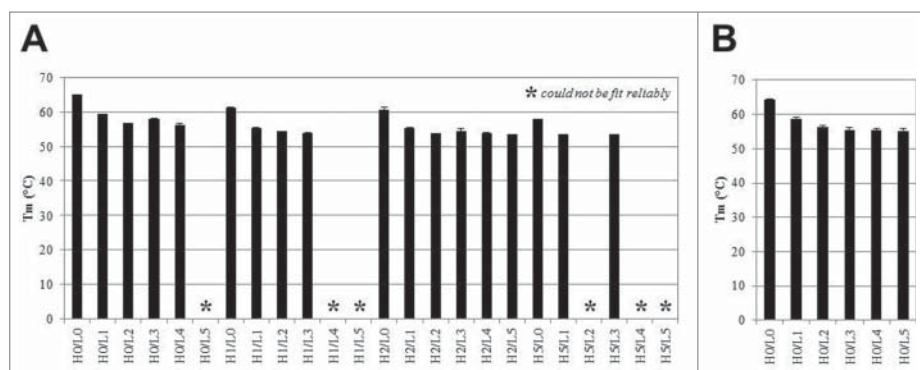
Figure 4. Thermostability of CAT192 Insertion Mutants Determined by DSF. (A) T_m values of heavy and light chain combination Fab mutants measured in triplicate, and (B) T_m values of CAT192 IgG4 light chain variants measured in triplicate at two concentrations and two dye: protein ratios.
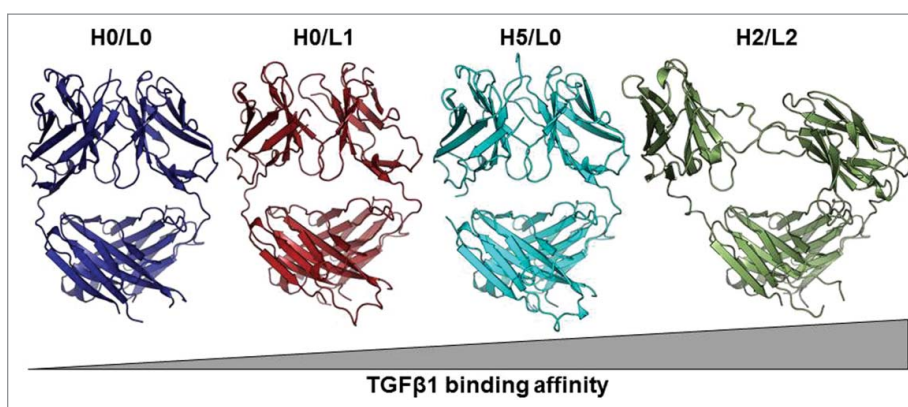
Figure 5. Crystal structures of CAT192 Fab constructs. The structures are ordered from lowest binding affinity (left) to highest binding affinity (right) for TGFβ1.

elbow region. Also, a trade off was observed between stability and affinity. As the number of residues inserted for each individual chain increased, a decrease was observed in the melting temperature. This may be due to reduced stabilization of the CH1/CL domains.

To confirm that this increase in binding affinity was due to increased flexibility of the antibody's elbow region, the structures were solved for select mutants. Wild type CAT192 Fab superimposed with similar low R.M.S.D. values to the H0/L1 and H5/L0, indicating high structure similarity. The H2/L2 variant superimposed with WT with a much higher R.M.S.D. than either of the previous variants, demonstrating a much larger conformational change between the constructs. Accordingly, an increase in R.M.S.D. correlated with an increase in binding affinity to TGFβ1. Since binding affinity and structural change show a direct correlation, this suggests the antibody must undergo considerable conformational arrangement to accommodate antigen binding. This change can occur by

displacement of variable domains or rearrangement of CDR loops. With an increase in elbow angle rotation due to increase in length and flexibility, the variable domains can adopt a larger range of conformations.

The fact that variable domains are spaced much more apart in H2/L2, and this mutant binds TGFβ1 with the highest affinity, suggests at least two possibilities. The first possibility is that the epitope on TGFβ1 is more elongated than the WT CAT192 can accommodate. Only when the elbow region is relaxed can the variable domains adopt the conformation needed to encompass this large epitope. This is why wild-type CAT192, even though it has the same CDR sequences as the H2/L2 variant, would bind with the lowest affinity: the molecule's restricted elbow region does not allow it to adopt the conformation needed for binding. When the elbow region was engineered to accommodate more flexibility, high affinity binding to TGFβ1 retained. The second possibility is that only one chain participates in the binding and the second chain is
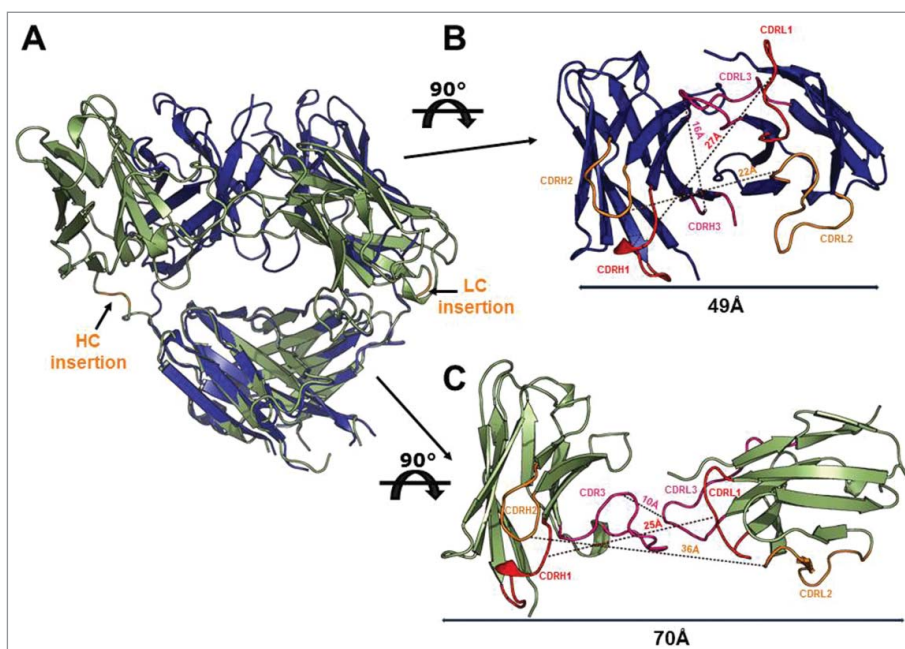
Figure 6. Superposition of WT CAT192 Fab and H2/L2 variant. (A) Wild type (blue) and H2/L2 (green) superimposed on the constant light chain. The heavy chain and light chain insertions in H2/L2 are shown in orange. (B) Top view of wild type CAT192 variable domain with each CDR colored (red: CDR1, orange: CDR2, pink: CDR3). (C) Top view of CAT192 H2/L2 with the same CDR color scheme as (B). The CDR distances were measured between HC Y32-LC G28 (CDR1), HC Y53-LC G60 (CDR2), and HC E101-LC Y94 (CDR3).
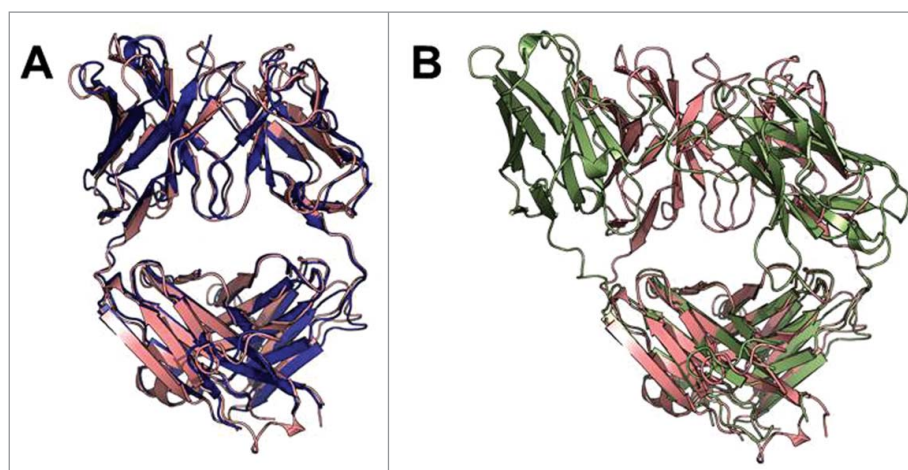
Figure 7. Superposition of fresolimumab (PDB:4KXZ, pink) with (A) wild type CAT192 Fab (blue) or (B) CAT192 H2/L2 Fab (green).

sterically hindering the binding interaction. When the elbow region sequence is longer, it allows the inhibitory chain to essentially move out of the way for antigen binding.

Fresolimumab is a pan-specific TGFβ antibody. High-resolution structures of the scFv or Fab forms fresolimumab bound to all three TGFβ isoforms have been determined.[14,20] Wild type CAT192, H0/L1, and H5/L0 show the most similarity with fresolimumab, and superimpose with similar R.M.S.D. values of 3.806 Å, 3.816 Å, and 3.877Å, respectively. In contrast, the H2/L2 variant superposition has a higher R.M.S.D. of 4.909 Å (Fig. 7). We know CAT192 H2/L2 must bind TGFβ1 in a different way than fresolimumab since WT CAT192 (which has the highest similarity to fresolimumab) does not bind TGFβ1 with high affinity. Size-exclusion chromatography combined with multi-angle light scattering (SEC-MALS) was run to understand what molar ratio CAT192 H2/L2 binds to TGFβ1. The complex elutes at a molecular weight of 129.6 kDa, corresponding to the weight of one TGFβ1 dimer with 2 Fab molecules (data not shown). This is the same stoichiometry as fresolimumab; thus, CAT192 H2/L2 must have a different epitope or mechanism of action.

Our results suggest that conformational changes in therapeutic antibodies could have an effect on binding affinity in general, and thus need to be carefully examined. This case study shows that inserting linker residues in the elbow region of the converted Fab and IgG molecule increases flexibility, and thus affinity. Our work demonstrates the benefits of structural and functional re-examination when converting scFv to IgG molecules and highlights the potential of structure-based engineering to produce fully functional antibodies.

Materials and methods

Construction and expression of CAT192 variants

CAT192 Fab and IgG4 expression plasmids were constructed by cloning the variable heavy and light chain sequences from CAT192 into the episomal expression vector, pFF.[21] The DNA sequences were ordered from GeneArt after optimizing for HEK293 expression. A six residue His-tag was added to the HC of the Fab for purification purposes. Primers were designed and ordered from Invitrogen. The QuikChange Lightning Site-Directed Mutagenesis Kit (Agilent) was used to add one glycine (G), two glycines (GG), two glycines and one serine (GGS), three glycines and one serine (GGGS), or four glycines and one serine (GGGGS) sequences into the CAT192 wild type LC or HC elbow region. All plasmid DNA was prepared with Qiagen kits and sequences were confirmed. The CAT192 LC or HC variants were co-expressed using the Expi293F transfection systems (Life Technologies) and conditioned media was harvested 4 days post-transfection. Expression in conditioned media was analyzed using an Octet QK384 biosensor (Pall FortéBio).

Purification of CAT192 Fab variants for TGFβ binding assessment

The CAT192 Fab variants in conditioned media were purified using PureSpeed IMAC tips (Rainin). The resin was equilibrated and washed in 10 mM sodium phosphate pH 7.4, 300 mM NaCl, 3 mM imidazole, and the protein was eluted in 10 mM sodium phosphate pH 7.4, 300 mM NaCl, 250 mM imidazole pH 7.4. The samples were buffer exchanged using Amicon Ultra filters (Millipore) into Gibco phosphate-buffered saline (PBS) pH 7.2 (Invitrogen) after the elution step.

Purification of CAT192 IgG variants for affinity and potency characterization

The CAT192 IgG4 variants were purified from conditioned media using Hi-Trap Protein A HP columns (GE Healthcare) with a peristaltic pump. The columns were equilibrated and washed with 50 mM sodium phosphate, 25 mM NaCl pH 7.1. A more stringent wash was performed in 10 mM sodium succinate pH 6.0, and the proteins were eluted in 10 mM sodium succinate pH 3.75. The eluates were neutralized with 0.2 M sodium hydroxide, and 0.2 M NaCl was added for a final concentration of 40 mM NaCl. The samples were then concentrated and buffer exchanged into 50 mM sodium phosphate, 25 mM NaCl pH 7.1 using Amicon Ultra filters (Millipore).

Surface plasmon resonance biosensor analysis

The Biacore T200 instrument (GE Healthcare) was used to assess the TGFβ binding affinity of the purified CAT192 WT and mutants. TGFβ1 and TGFβ2 were prepared and purified according to previously published procedures.[22,23] TGFβ3 was purchased from R&D Systems. Each isoform was immobilized to a CM5 series S chip using the amine coupling kit (GE Healthcare). To determine the binding affinities, low density chips were prepared in order to minimize avidity effects from binding to the immobilized TGFβ homodimers. High-density chips were prepared to compare CAT192 WT binding. CAT192 (metelimumab) was tested in early experiments (Fig. 1B and Supplementary Fig. 1C) and the CAT192 IgG4 S228P construct was used for all other analysis. The S228P mutation was used to reduce Fab arm exchange.[24] CAT192 WT and mutant Fabs or antibodies were always diluted the in HBS-EP+ running buffer (GE Healthcare). The surface was regenerated with 40 mM HCl as described previously.[14] Binding sensorgrams were fit to a 1:1 binding model using the BiaEvaluation software (GE Healthcare) or Scrubber (BioLogic Software) to calculate binding affinities.

Cell potency assay

The CAT192 insertion mutants were characterized in an *in vitro* potency assay as described previously.[15] TGFβ-induced interleukin-11 (IL-11) release from A549 human lung epithelial cells (ATCC) was measured by ELISA in this bioassay. IL-11 production was neutralized by anti-TGFβ antibodies. Briefly, WT CAT192 and mutants were serially diluted 10-fold in growth/assay medium in a 96-well plate for final concentrations of 0.5 pg/mL to 50 μg/mL in duplicate. TGFβ1 was then added to all of the wells to a final concentration of 0.3 ng/mL or 1 ng/mL and incubated in a 37°C humidified tissue culture incubator for 1 hour. The TGFβ1/CAT192 solution was then added to plated A549 cells and returned to the incubator overnight. An ELISA was then performed on the cell supernatants using an in-house human IL-11 ELISA to measure cytokine levels.

Differential scanning fluorimetry analysis

The Fab or IgG molecules were diluted to 0.1 mg/mL or 0.25 mg/mL in PBS pH 7.2 in duplicate and mixed with Sypro orange dye (Invitrogen) at a 1:4000 or 1:2000 dye ratio. The samples were heated from 20 to 100°C at a rate of 5°C/min using a CFX96 Real-Time PCR system (Bio-Rad). The T_m values were calculated using the Bio-Rad CFX Manager 3.0 software.

Purification of CAT192 Fab variants for structure determination

The CAT192 Fab variants in conditioned media were purified using a HisTrap excel column (GE Healthcare) equilibrated with 20 mM sodium phosphate pH 7.4, 500 mM NaCl, 5 mM imidazole. Proteins were eluted with 20 mM sodium phosphate pH 7.4, 500 mM NaCl, 500 mM imidazole and immediately buffer exchanged into 20 mM HEPES pH 7.0, 50 mM NaCl over a size exclusion chromatography column (Superdex 200 10/300 GL; GE Healthcare) as a final preparative step for crystal trials.

Crystallization and structure determination of CAT192 Fab variants

The CAT192 variants were concentrated to 20 mg/mL and sparse matrix screens were set-up using the sitting drop vapor diffusion method. Each variant crystallized at 4°C and in a different condition (Table 3). Crystals were cryo-protected in either 20% ethylene glycol (WT, H0/L1, H5/L0) or a gradient of 10–60% supersaturated lithium sulfate diluted in the mother liquor (H2/L2). All data sets were collected with a Rigaku FRE+ SuperBright generator and Saturn 944+ CCD detector and processed with iMosflm followed by Scala in the CCP4 package.[25,26] Wild-type CAT192 Fab was solved first and used 4G5Z HC & 3SKJ LC as search models for molecular replacement in Phaser.[27] The rest of the constructs used the WT CAT192 structure as a molecular placement model. Iterative model building and refinement were performed using phenix. refine and Coot.[28,29] Statistics of the structure are summarized in Table 3. All R.M.S.D values and atomic distances were calculated using PyMOL. Software used in this project was accessed through the SBGrid consortium.[30] Atomic coordinates have been deposited in the Protein Data Bank under accession codes 6AMJ (WT CAT192 Fab), 6AMM (H0/L1), 6ANP (H5/L0), and 6AO0 (H2/L2).

SEC-MALS

The molar mass of the CAT192 H2/L2:TGFβ1 complex was determined using SEC-MALS (WYATT miniDAWN Treos MALS device and Optilab rEX). The column (Superdex 200 10/300 GL; GE Healthcare) was equilibrated with 20 mM sodium acetate pH 5.0, 50 mM NaCl. To form the complex, CAT192 H2/L2 was added to TGFβ1 in a 2:1 ratio and incubated at 4°C overnight. Data were evaluated using the software ASTRA 6.1.

ORCID

Dana M. Lord http://orcid.org/0000-0001-9060-1210
Julie J. Bird http://orcid.org/0000-0002-0633-287X
Anna Park http://orcid.org/0000-0002-6511-8363
Ronnie R. Wei http://orcid.org/0000-0003-3606-6055

References

1. Hata A, Chen YG. TGF-beta Signaling from Receptors to Smads. Cold Spring Harb Perspect Biol. 2016;8. doi:10.1101/cshperspect.a022061

2. Fernandez IE, Eickelberg O. The impact of TGF-beta on lung fibrosis: from targeting to biomarkers. Proc Am Thor Soc. 2012;9:111–6. doi:10.1513/pats.201203-023AW

3. Lijnen PJ, Petrov VV, Fagard RH. Induction of cardiac fibrosis by transforming growth factor-beta(1). Mol Genet Metab. 2000;71:418–35. doi:10.1006/mgme.2000.3032

4. Kubiczkova L, Sedlarikova L, Hajek R, Sevcikova S. TGF-beta – an excellent servant but a bad master. J Transl Med. 2012;10:183. doi:10.1186/1479-5876-10-183

5. Hawinkels LJ, Ten Dijke P. Exploring anti-TGF-beta therapies in cancer and fibrosis. Growth Factors. 2011;29:140–52. doi:10.3109/08977194.2011.595411

6. Attisano L, Wrana JL. Signal transduction by members of the transforming growth factor-beta superfamily. Cytokine & Growth Factor Rev. 1996;7:327–39. doi:10.1016/S1359-6101(96)00042-1

7. Denton CP, Merkel PA, Furst DE, Khanna D, Emery P, Hsu VM, Silliman N, Streisand J, Powell J, Akesson A, et al. Recombinant human anti-transforming growth factor beta1 antibody therapy in systemic sclerosis: a multicenter, randomized, placebo-controlled phase I/II trial of CAT-192. Arthritis Rheum. 2007;56:323–33. doi:10.1002/art.22289

8. Stanfield RL, Takimoto-Kamimura M, Rini JM, Profy AT, Wilson IA. Major antigen-induced domain rearrangements in an antibody. Structure. 1993;1:83–93. doi:10.1016/0969-2126(93)90024-B

9. Bhat TN, Bentley GA, Fischmann TO, Boulot G, Poljak RJ. Small rearrangements in structures of Fv and Fab fragments of antibody D1.3 on antigen binding. Nature. 1990;347:483–5. doi:10.1038/347483a0

10. Herron JN, He XM, Ballard DW, Blier PR, Pace PE, Bothwell AL, Voss EW Jr, Edmundson AB. An autoantibody to single-stranded DNA: comparison of the three-dimensional structures of the unliganded Fab and a deoxynucleotide-Fab complex. Proteins. 1991;11:159–75. doi:10.1002/prot.340110302

11. Landolfi NF, Thakur AB, Fu H, Vasquez M, Queen C, Tsurushita N. The integrity of the ball-and-socket joint between V and C domains is essential for complete activity of a humanized antibody. J Immunol. 2001;166:1748–54. doi:10.4049/jimmunol.166.3.1748

12. Shen Z, Yan H, Zhang Y, Mernaugh RL, Zeng X. Engineering peptide linkers for scFv immunosensors. Anal Chem. 2008;80:1910–7. doi:10.1021/ac7018624

13. Stanfield RL, Zemla A, Wilson IA, Rupp B. Antibody elbow angles are influenced by their light chain class. J Mol Biol. 2006;357:1566–74. doi:10.1016/j.jmb.2006.01.023

14. Moulin A, Mathieu M, Lawrence C, Bigelow R, Levine M, Hamel C, Marquette JP, Le Parc J, Loux C, Ferrari P, et al. Structures of a pan-specific antagonist antibody complexed to different isoforms of TGFbeta reveal structural plasticity of antibody-antigen interactions. Protein sci: a publication of the Protein Society. 2014;23:1698–707. doi:10.1002/pro.2548

15. Rapoza ML, Fu D, Sendak RA. Development of an in vitro potency assay for therapeutic TGFbeta antagonists: the A549 cell bioassay. J Immunol Methods. 2006;316:18–26. doi:10.1016/j.jim.2006.07.009

16. Steinwand M, Droste P, Frenzel A, Hust M, Dubel S, Schirrmann T. The influence of antibody fragment format on phage display based affinity maturation of IgG. mAbs. 2014;6:204–18. doi:10.4161/mabs.27227

17. Mazor Y, Van Blarcom T, Carroll S, Georgiou G. Selection of full-length IgGs by tandem display on filamentous phage particles and Escherichia coli fluorescence-activated cell sorting screening. FEBS J. 2010;277:2291–303. doi:10.1111/j.1742-4658.2010.07645.x

18. Chan CE, Chan AH, Lim AP, Hanson BJ. Comparison of the efficiency of antibody selection from semi-synthetic scFv and non-immune Fab phage display libraries against protein targets for rapid development of diagnostic immunoassays. J Immunol Methods. 2011;373:79–88. doi:10.1016/j.jim.2011.08.005

19. Schirrmann T, Meyer T, Schutte M, Frenzel A, Hust M. Phage display for the generation of antibodies for proteome research, diagnostics and therapy. Molecules. 2011;16:412–26. doi:10.3390/molecules16010412

20. Grutter C, Wilkinson T, Turner R, Podichetty S, Finch D, McCourt M, Loning S, Jermutus L, Grütter MG. A cytokine-neutralizing antibody as a structural mimetic of 2 receptor interactions. Proc Natl Acad Sci U S A. 2008;105:20251–6. doi:10.1073/pnas.0807200106

21. Steinmetz A, Vallee F, Beil C, Lange C, Baurin N, Beninga J, Capdevila C, Corvey C, Dupuy A, Ferrari P, et al. CODV-Ig, a universal bispecific tetravalent and multifunctional immunoglobulin format for medical applications. mAbs. 2016;8:867–78. doi:10.1080/19420862.2016.1162932

22. Schlunegger MP, Cerletti N, Cox DA, McMaster GK, Schmitz A, Grutter MG. Crystallization and preliminary X-ray analysis of recombinant human transforming growth factor beta 2. FEBS lett. 1992;303:91–3. doi:10.1016/0014-5793(92)80484-X

23. Hinck AP, Archer SJ, Qian SW, Roberts AB, Sporn MB, Weatherbee JA, Tsang ML, Lucas R, Zhang BL, Wenker J, et al. Transforming growth factor beta 1: three-dimensional structure in solution and comparison with the X-ray structure of transforming growth factor beta 2. Biochemistry. 1996;35:8517–34. doi:10.1021/bi9604946

24. van der Neut Kolfschoten M, Schuurman J, Losen M, Bleeker WK, Martinez-Martinez P, Vermeulen E, den Bleker TH, Wiegman L, Vink T, Aarden LA, et al. Anti-inflammatory activity of human IgG4 antibodies by dynamic Fab arm exchange. Science. 2007;317:1554–7. doi:10.1126/science.1144603

25. Battye TG, Kontogiannis L, Johnson O, Powell HR, Leslie AG. iMOSFLM: a new graphical interface for diffraction-image processing with MOSFLM. Acta Crystallogr D, Biol Crystallogr. 2011;67:271–81. doi:10.1107/S0907444910048675

26. Winn MD, Ballard CC, Cowtan KD, Dodson EJ, Emsley P, Evans PR, Keegan RM, Krissinel EB, Leslie AG, McCoy A, et al. Overview of the CCP4 suite and current developments. Acta Crystallogr D, Biol Crystallogr. 2011;67:235–42. doi:10.1107/S0907444910045749

27. McCoy AJ, Grosse-Kunstleve RW, Adams PD, Winn MD, Storoni LC, Read RJ. Phaser crystallographic software. J Appl Crystallogr. 2007;40:658–74. doi:10.1107/S0021889807021206

28. Adams PD, Afonine PV, Bunkoczi G, Chen VB, Davis IW, Echols N, Headd JJ, Hung LW, Kapral GJ, Grosse-Kunstleve RW, et al. PHENIX: a comprehensive Python-based system for macromolecular structure solution. Acta Crystallogr D, Biol Crystallogr. 2010;66:213–21. doi:10.1107/S0907444909052925

29. Emsley P, Lohkamp B, Scott WG, Cowtan K. Features and development of Coot. Acta Crystallogr D, Biol Crystallogr. 2010;66:486–501. doi:10.1107/S0907444910007493

30. Morin A, Eisenbraun B, Key J, Sanschagrin PC, Timony MA, Ottaviano M, Sliz P. Collaboration gets the most out of software. eLife. 2013;2:e01456. doi:10.7554/eLife.01456